ACS Partner Journal
PRECISION CHEMISTRY

Open Access
This article is licensed under CC-BY-NC-ND 4.0

pubs.acs.org/PrecisionChem
Article

Supported Cu/Ni Bimetallic Cluster Electrocatalysts Boost CO_2 Reduction

Depeng Wang, Jiazhi Wang, Zhi Wang, Ning Zhang, Jianrong Zeng, Haixia Zhong,* and Xinbo Zhang*

Cite This: *Precis. Chem.* 2024, 2, 96−102
Read Online

ACCESS | Metrics & More | Article Recommendations | Supporting Information

ABSTRACT: Supported metal clusters with the integrated advantages of single-atom catalysts and conventional nanoparticles held great promise in the electrocatalytic carbon dioxide reduction (ECO_2R) operated at low overpotential and high current density. However, its precise synthesis and the understanding of synergistically catalytic effects remain challenging. Herein, we report a facile method to synthesize the bimetallic Cu and Ni clusters anchored on porous carbon (Cu/Ni−NC) and achieve an enhanced ECO_2R. The aberration-corrected high-angle annular dark-field scanning transmission electron microscopy and synchrotron X-ray absorption spectroscopy were employed to verify the metal dispersion and the coordination of Cu/Ni clusters on NC. As a result of this route, the target Cu/Ni−NC exhibits excellent electrocatalytic performance including a stable 30 h electrolysis at 200 mA cm^{-2} with carbon monoxide Faradaic efficiency of ~95.1% using a membrane electrode assembly electrolysis cell. Combined with the in situ analysis of the surface-enhanced Fourier transform infrared spectroelectrochemistry, we propose that the synergistic effects between Ni and Cu can effectively promote the H_2O dissociation, thereby accelerate the hydrogenation of CO_2 to *COOH and the overall reaction process.

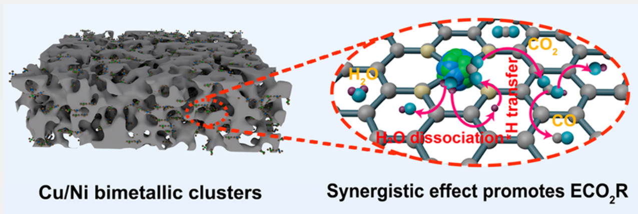

KEYWORDS: *electrocatalytic CO_2 reduction, bimetallic cluster, synergistic catalysis, membrane electrode assembly electrolysis cell, in situ surface-enhanced infrared absorption spectroscopy*

INTRODUCTION

Electrocatalytic carbon dioxide reduction (ECO_2R) into chemical feedstocks, driven by the renewable electricity, point a new path out to turn CO_2 into valuable products for the sustainable carbon loop while storing energy.[1] Among various ECO_2R products, CO is one of the most important products, which has been widely used as the crucial feedback, such as Fischer−Tropsch industries.[2] However, the activity and selectivity of ECO_2R are seriously restricted by the chemically inert feature of CO_2 and the kinetically efficient competing reaction of hydrogen evolution.[3] Therefore, lots of research has been triggered in developing robust electrocatalysts to facilitate the kinetics of ECO_2R to CO for meeting the industrial requirements with high reaction rate and high selectivity. In the past years, a variety of ECO_2R catalysts have been reported, including noble metal catalysts (Ag,[4] Au,[5] and Pd[6]), molecular catalysts (metal porphyrins[7] and metal phthalocyanines[8]), and single-atom catalysts (SACs).[9−11] Even then, it is far behind the practical demand since the challenges still lie in the development of earth-abundant and efficient catalytic materials and in-depth analysis of reaction mechanisms.

SACs have been attached great attentions in ECO_2R due to the nearly 100% accessible active site and controllable metal coordination environment.[12] Particularly, Ni SACs have exhibited large current density (j) and high carbon monoxide Faradaic efficiency (FE_{CO}) through many effective strategies, such as tailoring the coordination number of Ni atom,[13] heteroatom doping,[14] etc. However, the sluggish reaction process of proton-coupled electrons transfer at the active site of single Ni atom largely limits the overall reaction rate.[15] Introducing another metal was explored to break the limited linear relationship between the adsorption of reaction intermediates and the catalytic activity on single catalytic sites, thus improving the catalytic performance.[16] For instance, Chen et al.[17] reported Ni−Cu diatomic site catalysts can reduce the formation energy of the key *COOH intermediate via the synergistic effect between Cu and Ni. Besides, diatomic Ni−Fe bimetallic active centers were also able to promote the hydrogenation of CO_2 to COOH* and the release of CO.[18] Overall, the synergistic effect between two metallic sites is conducive to optimizing the formation and desorption of key intermediates during the ECO_2R process. Additionally, metal clusters like Ni nanoclusters (NiN_x) immobilized on N-doped carbon nanotubes (NCNT) is found to be more active for

Received: October 22, 2023
Revised: February 1, 2024
Accepted: February 2, 2024
Published: March 4, 2024

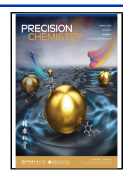

Downloaded via CHANGCHUN INST OF APPLIED CHEMISTRY on March 26, 2024 at 01:16:48 (UTC).
See https://pubs.acs.org/sharingguidelines for options on how to legitimately share published articles.

ACS Publications
© 2024 The Authors. Co-published by University of Science and Technology of China and American Chemical Society

https://doi.org/10.1021/prechem.3c00101
Precis. Chem. 2024, 2, 96−102

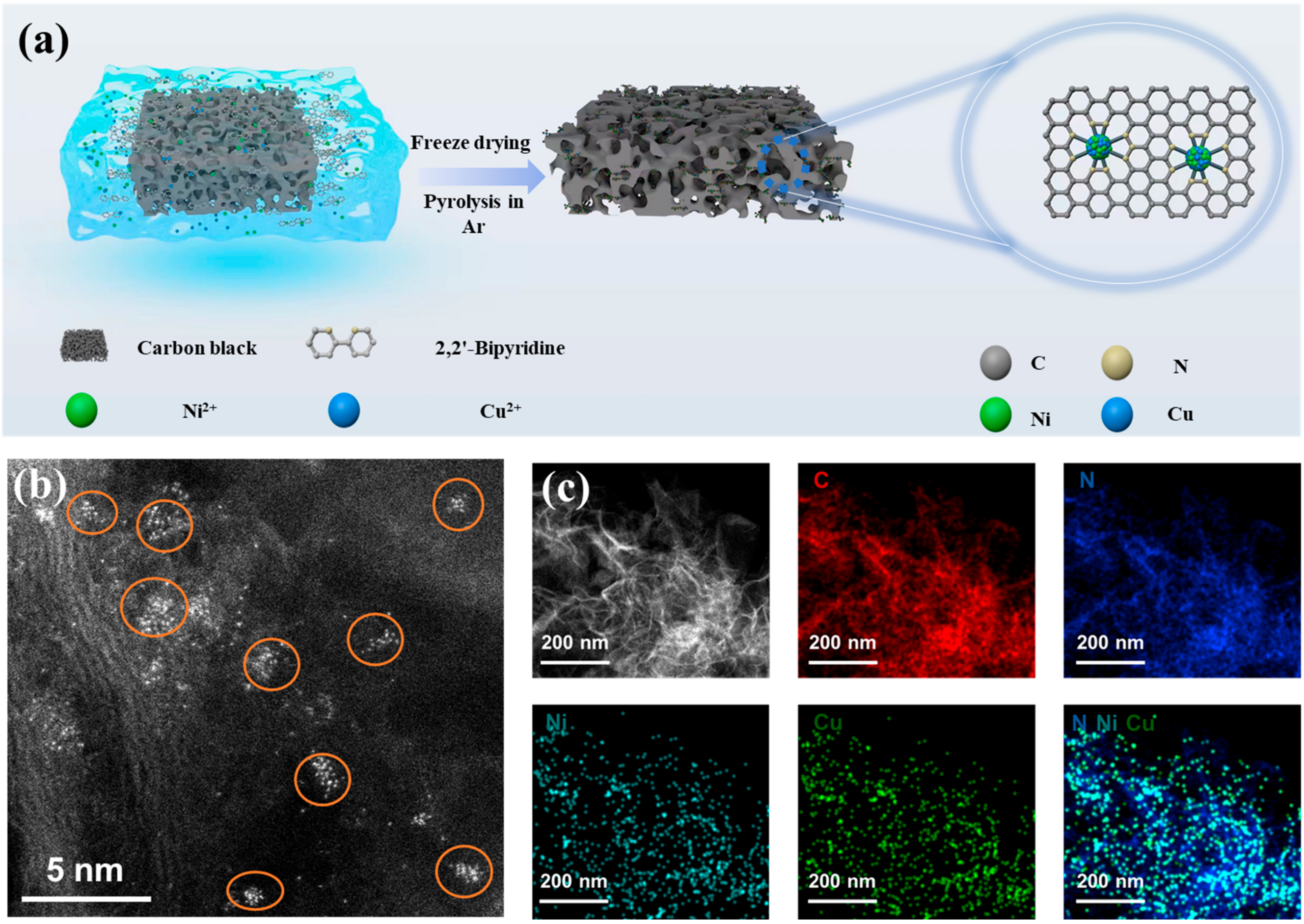

Figure 1. Synthesis and morphology characterization. (a) Schematic illustration of Cu/Ni−NC synthesis. (b) HAADF-STEM image of Cu/Ni−NC. (c) EDS (energy dispersive spectrometer) mappings of C, N, Cu and Ni elements of Cu/Ni−NC.

ECO_2R owing to a lower Gibbs free energy to form *COOH than the Ni single sites as well.[19] In this context, bimetallic cluster catalysts can offer more opportunities in achieving high catalytic performance by virtue of their more abundant metal active sites and the possible synergistic effects on generating and stabilizing the key intermediate species during the ECO_2R process. Therefore, the development of rational supported bimetallic cluster catalyst in boosting the ECO_2R and the deep insight into the synergistic role of each metal is expected; however, it remains grand challenging.

Herein, we report a facile method to synthesize atomically dispersed bimetallic copper and nickel cluster catalysts (Cu/Ni−NC) in electrocatalytic ECO_2R to CO and an understanding of the synergistic contribution of Cu and Ni to the achieved high electrochemical performance. The Aberration-corrected high-angle annular dark-field scanning transmission electron microscopy (HAADF-STEM) and the synchrotron X-ray absorption spectroscopy (XAS) analysis identified the metal dispersion state and coordination on the carbon subtract. Compared with the atomically dispersed copper cluster catalyst (Cu−NC) and atomically dispersed nickel cluster catalyst (Ni−NC) counterpart, Cu/Ni−NC exhibits higher activity with the j_{CO} of 19 mA cm^{-2} and FE_{CO} of ~93.2% at −0.7 V versus reversible hydrogen electrode (vs RHE) in H-cell. Moreover, we used membrane electrode assembly (MEA) cell to further evaluate the catalytic performance of the catalyst close to the practical application, which can stably work over 30 h (j = 200 mA cm^{-2}), outputting high CO selectivity of FE_{CO} over 95.1% and the cell voltage of 2.98 V. In-situ characterization suggests that the synergistic effects of Ni and Cu play an important role in promoting the H_2O dissociation, which favors the rapid CO_2 hydrogenation to *COOH and accelerating the overall reaction. This work provides a facile synthesis method for the atomically dispersed non-noble metal cluster catalysts and also provides a basic effective strategy in constructing efficient ECO_2R and other complex reactions.

■ RESULTS AND DISCUSSION

Synthesis and Characterizations

As shown in Figure 1a, Cu/Ni−NC was obtained via a cascade anchoring strategy. First, nitrogen doped carbon (NC) substrate with high specific surface area was synthesized by the carbonization of the cheap chitosan precursor, where high specific surface area facilitates the exposure of more accessible active site and the sufficient transfer of the reactants and products.[20] Then, Cu/Ni−NC was obtained by the pyrolysis of the precursors of copper nitrate, nickel nitrate, and 2,2′-Dipyridine on NC, acidic washing and drying overnight. Powder X-ray diffraction (XRD) pattern (Figure S1) shows only one broad diffraction peaks at 25.2° for Cu/Ni−NC, which is assigned to the crystal face (002) of graphitic carbon, excluding the presence of crystalline metal particles on NC supports.[21] HAADF-STEM was further performed to verify the dispersion state of the Ni and Cu elements on carbon substrates. As shown in Figure 1b, numerous bright spots were observed for

Cu/Ni−NC in the dark field condition, which can be attributed to the metal atoms of Cu and Ni due to its greater contrast under dark field condition,[20] indicating that the metal atoms exist as clusters on carbon substrates. Elemental mappings (Figure 1c) proven the even distribution of Ni, Cu and N elements over the carbon substrates. Similarly, as identified by the XRD pattern (Figure S1) and electron microscopy analysis (Figures S2 and S3), atomically Ni and Cu clusters exist in the Ni−NC and Cu−NC counterpart, respectively, which were synthesized with the same approach.

The specific surface area and pore size structure of the prepared catalysts were analyzed by nitrogen adsorption and desorption isotherms. The specific surface area of Cu/Ni−NC is calculated up to 2681 m^2 g^{-1} (Figure S4), which is favorable for exposing abundant accessible active site and the mass transfer of the gas during the reaction process.[20] Meanwhile, a significant hysteresis loop structure in the adsorption and desorption curves implies the mesoporous structure of Cu/Ni−NC. Furthermore, the pore size distribution analysis identifies the existence of many micropores and mesopores for Cu/Ni−NC with the pore size range from 0.5 to 6 nm. This constructed micromesoporous structure is conducive to the sufficient mass transfer during the catalytic reaction.[22] In addition, Ni−NC and Cu−NC also have similar specific surface areas and pore structures compared to Cu/Ni−NC. The contents of metal elements in these catalysts were determined by inductively coupled plasma-optical emission spectroscopy (ICP, Table S1). Cu and Ni contents in Cu/Ni−NC were similar. Notably, all these prepared catalysts possess the superhydrophobic surface as their contact angle for the prepared catalysts were above 150° (Figure S5), which mitigated the flooding of the gas-diffusion electrode and increased the concentration of CO_2 at the electrode interface.[7,22]

X-ray photoelectron spectroscopy (XPS) and synchrotron XAS characterization were undertaken to investigate the chemical states and atomic-scale configurations of Cu and Ni for the prepared samples. The N 1s XPS spectra of all these catalysts were consistently deconvoluted into four N species (pyridinic N: 398.5 eV, graphitic N: 401.3 eV, metal N: 400.2 eV, oxidized N: 403.7 eV).[17] The high-resolution Cu and Ni 2p XPS spectra indicates that Ni and Cu valence is between 0 and +2, which is possibly due to the presence of nitrogen coordinated metal of the prepared catalyst (Figures S6−S8).[19] Figure 2a and 2c illustrates the X-ray near-edge structure (XANES) spectra at Ni/Cu K-edge for the prepared samples of Cu/Ni−NC, Ni−NC and the standard samples of the metal (Ni and Cu) foil and metal phthalocyanine (NiPC/CuPC). The absorption edge position of Ni for both Cu/Ni−NC and Ni−NC is located between the Ni foil and NiPC, further illustrating that the average Ni/Cu valence state is between 0 and +2. The absorption edge of Ni for Cu/Ni−NC is slightly shifted compared to Ni−NC, which suggest that the introduced Cu atoms affects the electronic structure of Ni atoms on NC.[20] As Cu K-edge XANES (X-ray absorption near edge structure) spectra shown in Figure 2c, the similar phenomena was observed of Cu/Ni−NC and Cu−NC. The Fourier transforms of the extended X-ray absorption fine structure (FT-EXAFS) spectra for both Cu/Ni−NC, Ni−NC, metal foil, and metal phthalocyanine are displayed in Figure 2b

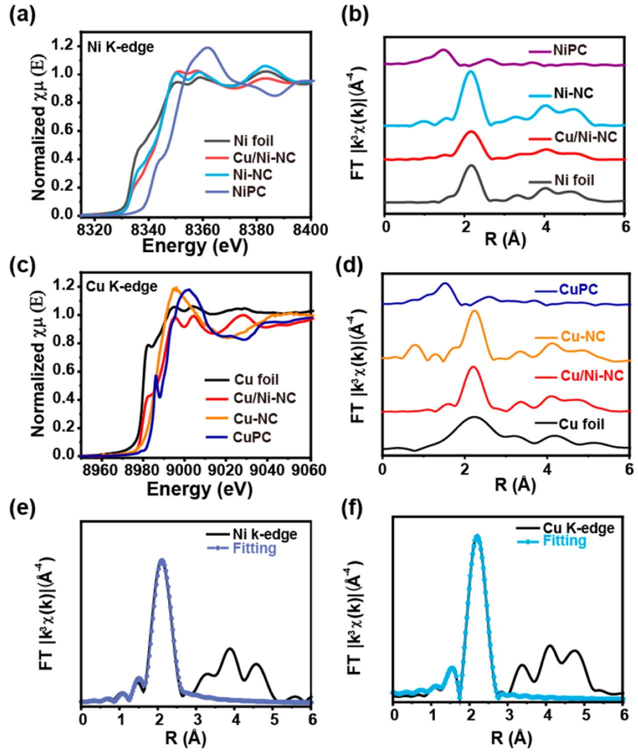

Figure 2. Structural characterization. (a, b) XANES spectra of Ni K-edge and FTs of k^3-weighted Ni K-edge EXAFS data for Cu/Ni−NC, Ni−NC, NiPC and Ni foil. (c, d) XANES spectra of Cu K-edge and FTs of k^3-weighted Cu K-edge EXAFS for Cu/Ni−NC, Cu−NC, CuPc and Cu foil. (d, e, f) Experimental and the fitting Ni and Cu K-edge EXAFS curves in R space of Cu/Ni−NC.

and 2d. Cu/Ni−NC and Ni−NC have similar peaks at ∼1.99 and ∼2.47 Å at Ni K-edge that are attributed to Ni−N and Ni−Ni (or Ni−Cu) paths. It is thus clear that Ni is dispersed atomically on nitrogen doped carbon substrates.[23] There are two peaks located at 1.91 and 2.49 Å, which are attributed to Cu−N and Cu−Cu (or Cu−Ni).[23] Furthermore, the local coordination structure of Cu/Ni−NC, Ni−NC, and Cu−NC was analyzed by the least-squares EXAFS curve fitting using the models with varied d values (Figure 2e-f and Figure S9). The detailed fitting results are shown in Table S2. Therefore, atomically dispersed bimetallic Cu/Ni−NC, Ni−NC, and Cu−NC are successfully synthesized.

ECO_2R Performance Evaluation

First, the ECO_2R performance of these control samples were evaluated in an H-cell using three-electrode system in CO_2-saturated electrolyte (0.5 M $KHCO_3$). The linear sweep voltammetry (LSV) curves of the prepared catalysts were displayed in Figure 3a. Compared with Ni−NC and Cu−NC, Cu/Ni−NC had a lower onset potential, indicating that Cu/Ni−NC had the better CO_2 activation ability. Moreover, Cu/Ni−NC exhibits the higher current density across the entire applied potential window than Cu−NC and Ni−NC. The electrochemical active surface area (ECSA) was compared by evaluating the double layer capacitance (C_{dl}) of these control catalysts (Figure S10).[24] The C_{dl} of Cu/Ni−NC (124.2 mF cm^{-2}) is larger than that of Ni−NC (103.6 mF cm^{-2}) and Cu−NC (89.3 mF cm^{-2}), which is likely due to that the synergistic effect between Cu and Ni provides more active sites.[23] Chronoamperometry was performed at the potential of

https://doi.org/10.1021/prechem.3c00101
Precis. Chem. 2024, 2, 96−102

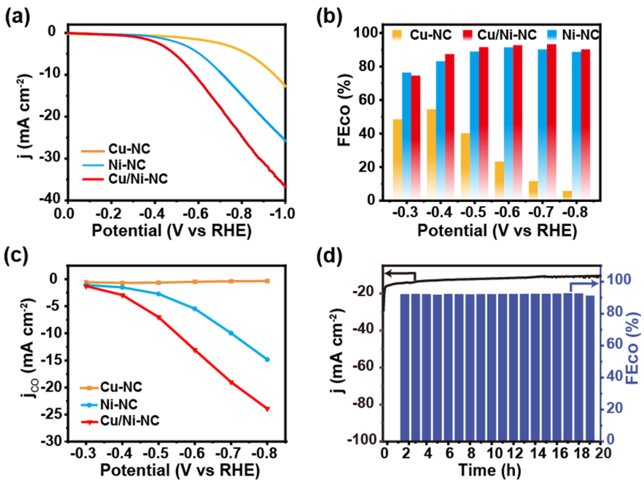

Figure 3. Electrocatalytic performance tested in H-cell. (a, b) LSV curves obtained in CO_2-saturated electrolyte (0.5 M $KHCO_3$) and FE_{CO} over different potentials of the as-fabricated Cu/Ni−NC, Ni−NC and Cu−NC. (c) j_{CO} of the as-fabricated samples under different potentials. (d) j and FE_{CO} vs the electrolysis time for Cu/Ni−NC electrode under −0.7 V vs RHE.

−0.3 to −0.8 V vs RHE. The gas products were examined by gas chromatography, and the liquid products were analyzed by ^{1}H-nuclear magnetic resonance (^{1}H NMR). As shown in Figure 3b, within the potential range, only CO and H_2 were detected. Cu/Ni−NC exhibits high CO selectivity with 93.2% of the maximum FE_{CO} at −0.7 V vs RHE. And the FE_{CO} of Cu/Ni−NC can be maintained over 85% from −0.4 to −0.8 V (vs RHE). Contrastively, the FE_{CO} of Ni−NC is only slightly lower than Cu/Ni−NC, along with the maximum FE_{CO} of 91.4% (−0.6 V vs RHE). The largest FE_{CO} of Cu−NC was only 55% (−0.4 V vs RHE). Besides, the CO partial current densities (j_{CO}) of these catalysts were compared at various application potentials, as shown in Figure 3c. The j_{CO} values of Cu/Ni−NC over the total applied potentials are obviously higher when compared to that of Ni−NC and Cu−NC. The above results claim that the introduction of Cu atoms significantly improves the catalytic activity of the Ni−NC catalyst.

The long-term catalytic durability of Cu/Ni−NC in H-cell was evaluated at −0.7 V vs RHE (Figure 3d). After the constant 20 h operations, the current density and the CO selectivity of Cu/Ni−NC did not decline apparently, and the liquid phase product in the electrolyte was not detected

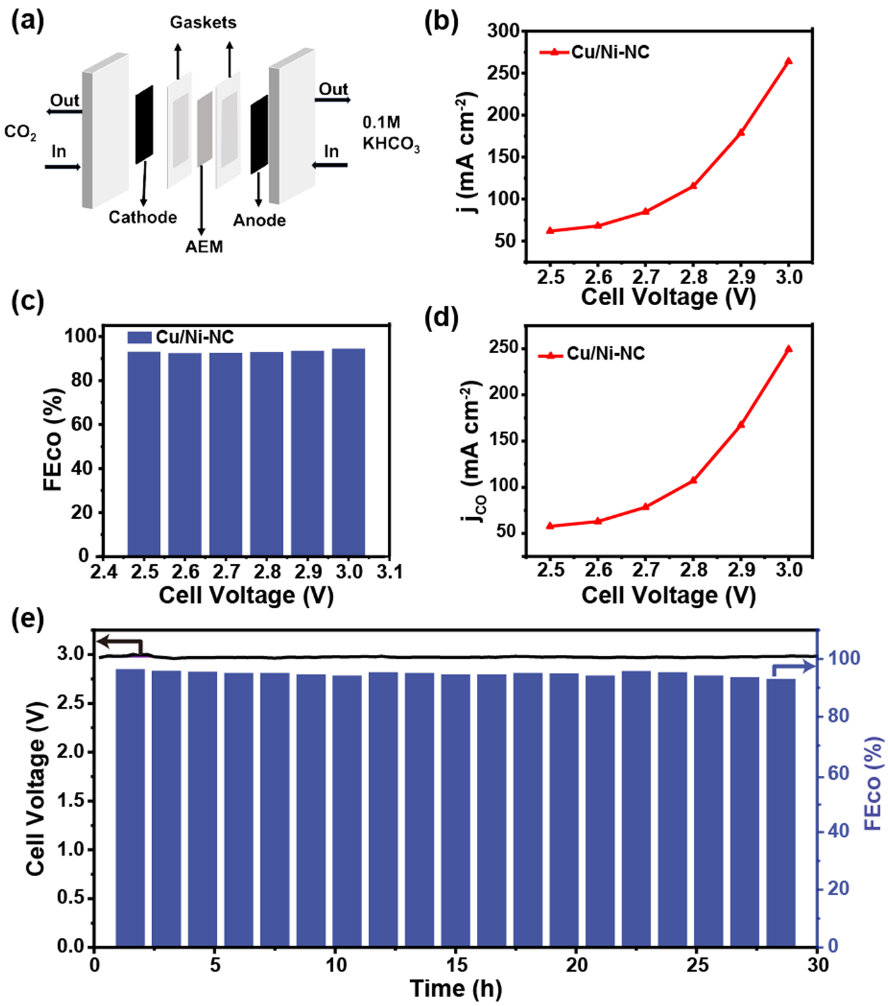

Figure 4. Electrocatalytic performance tested in a MEA electrolyzer. (a) Schematic illustration of the electrolysis device. (b) j of Cu/Ni−NC under different cell voltages. (c) FE_{CO} of Cu/Ni−NC under different cell voltages. (d) j_{CO} of Cu/Ni−NC under different cell voltages. (e) Stability of Cu/Ni−NC electrode under 200 mA cm^{-2}.

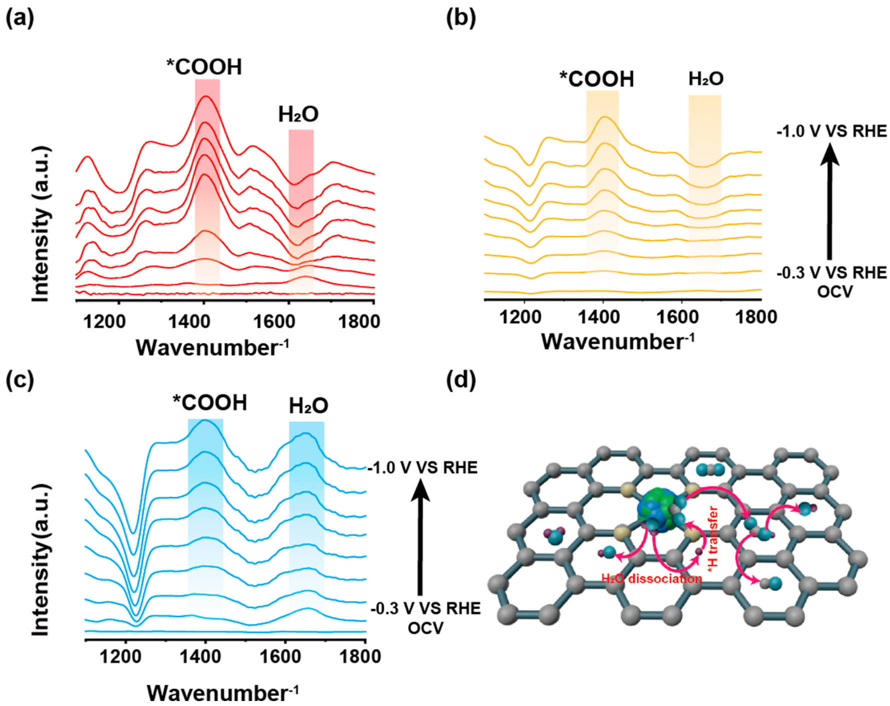

Figure 5. In situ ATR-SEIRAS recorded during ECO_2R (a) Cu/Ni−NC. (b) Cu−NC. (c) Ni−NC. (d) Proposed catalytic mechanism of Cu/Ni−NC for ECO_2R.

(Figure S11). Subsequently, Cu/Ni−NC, Ni−NC, and Cu−NC after 20 h of electrolysis were characterized by XRD and TEM. The XRD pattern of Cu/Ni−NC, Ni−N, Cu−NC and carbon paper is displayed in Figure S12. No obvious metal diffraction peaks were observed, excluding the formation of metal nanoparticles after long-term electrolysis, which is also further identified by the TEM images (Figures S13−15). Besides, Ni and Cu elements were uniform dispersed on the carbon substrate. Moreover, the electrolyte before and after 20 h electrolysis was examined by ICP atomic emission spectroscopy. Result shows that metal atom hardly leaches out during the electrolysis. Thus, it is demonstrated that the prepared catalysts have good stability during the ECO_2R.

Despite with advanced electrocatalysts, the low solubility and sluggish transport of CO_2 in aqueous electrolyte in H-cell will limit the increase of j.[22] To avoid these problems, the MEA electrolysis device was further utilized to estimate the catalytic contribution of Cu/Ni−NC at industrial-level current density. Figure 4a shows the MEA that was composed of the Cu/Ni−NC on a gas-diffusion electrode (GDE) as the cathode, the $IrO_2 \cdot xH_2O$ anode and an anion exchange membrane (AEM). Figure 4b displays the current density recorded at each applied voltage. Upon increasing the applied current density from 62 to 264 mA cm^{-2}, the voltage of the assembled MEA increase from 2.5 to 3.0 V, along with FE_{CO} up to 90% (Figure 4c). The j_{CO} increased from 57 to 250 mA cm^{-2} at the identical cell voltage (Figure 4d). Moreover, Cu/Ni−NC exhibits long-term durability in the MEA electrolyzer. As shown in Figure 4e, the Cu/Ni−NC maintains a high FE_{CO} of over 90% and the stable output voltage at 200 mA cm^{-2} under the long-term electrolysis for 30 h. Compared with other similar catalysts, the Cu/Ni−NC catalyst exhibits the advantages in the high-efficiency electrocatalytic ECO_2R regarding the electrolysis time, FE_{CO}, cell voltage and current density (Table S3).

Catalytic Process Analysis

The in situ surface-enhanced infrared absorption spectroscopy (ATR-SEIRAS) was measured to analyze the electrocatalytic ECO_2R process. Generally, it was found that the observed negative peak is associated with the consumed intermediates while a positive peak was resulted by the generated one intermediates.[25] The positive peak at 1403 cm^{-1} is associated with the adsorbed *COOH.[13] With the negative shift of the potential, this positive peak of the as-synthesized Cu/Ni−NC, Ni−NC and Cu−NC gradually reinforces, indicating an increased formation of *COOH on the catalyst surface (Figure 5a−c). As shown in Figure 5a, a negative peak located at 1620 cm^{-1} gradually reinforces upon the negative shift of the potential, which is attributed to the faster consumption of H_2O than the accumulation on the Cu/Ni−NC surface during the electrolysis process.[26] Similar phenomenon is also observed for Cu−NC (Figure 5b). Thus, the introduction of Cu benefits the dissociation of water, which are favorable for the hydrogenation reactions in the aqueous electrocatalysis.[14] Differently, only a positive peak nearly located at 1620 cm^{-1} appears for Ni−NC, of which the intensity increases with the negative shift of the potential. Thus, the adsorption of H_2O on the Ni−NC surface is dominant compared to the consumption of H_2O, resulting in the enrichment of H_2O on the catalyst surface. Based on the above analysis, it is proposed that the accelerated water dissociation through importing Cu promotes the electrochemical hydrogenation of CO_2 to the key intermediate *COOH and thus improve the overall electrocatalytic performance of Cu/Ni−NC catalysts compared with Ni catalysts (Figure 5d).

■ CONCLUSION

In this work, a convenient and universal method was adopted to successfully synthesize an atomic level dispersed bimetallic Cu and Ni catalyst. The Cu/Ni−NC exhibits better electro-

https://doi.org/10.1021/prechem.3c00101
Precis. Chem. 2024, 2, 96−102

catalytic performance compared with Ni−NC and Cu−NC. In MEA test, FE_{CO} up to 95.1% and the cell voltage of 2.98 V are obtained at 200 mA cm^{-2}. Combined with in situ ATR-SEIRAS analysis, we speculate that the improved electrocatalytic performance originates from the synergistic role of Cu and Ni: Cu helps accelerate the water dissociation and promote the CO_2 hydrogenation to *COOH on Ni sites. This work provides a convenient and universal strategy for fabricating the atomically dispersed metal cluster catalysts and emphasizes the synergistic effect of different metals in electrocatalytic complex reactions.

■ ASSOCIATED CONTENT

Supporting Information

The Supporting Information is available free of charge at https://pubs.acs.org/doi/10.1021/prechem.3c00101.

Material synthesis, physical characterizations, electrochemical measurements, and performance comparison (PDF)

■ AUTHOR INFORMATION

Corresponding Authors

Haixia Zhong − *State Key Laboratory of Rare Earth Resource Utilization, Changchun Institute of Applied Chemistry, Chinese Academy of Sciences, Changchun 130022, China; School of Applied Chemistry and Engineering, University of Science and Technology of China, Hefei 230026, China;* orcid.org/0000-0002-2839-0253; Email: hxzhong@ciac.ac.cn

Xinbo Zhang − *State Key Laboratory of Rare Earth Resource Utilization, Changchun Institute of Applied Chemistry, Chinese Academy of Sciences, Changchun 130022, China; School of Applied Chemistry and Engineering, University of Science and Technology of China, Hefei 230026, China;* orcid.org/0000-0002-5806-159X; Email: xbzhang@ciac.ac.cn

Authors

Depeng Wang − *State Key Laboratory of Rare Earth Resource Utilization, Changchun Institute of Applied Chemistry, Chinese Academy of Sciences, Changchun 130022, China; School of Applied Chemistry and Engineering, University of Science and Technology of China, Hefei 230026, China*

Jiazhi Wang − *State Key Laboratory of Rare Earth Resource Utilization, Changchun Institute of Applied Chemistry, Chinese Academy of Sciences, Changchun 130022, China; School of Applied Chemistry and Engineering, University of Science and Technology of China, Hefei 230026, China*

Zhi Wang − *State Key Laboratory of Rare Earth Resource Utilization, Changchun Institute of Applied Chemistry, Chinese Academy of Sciences, Changchun 130022, China; School of Applied Chemistry and Engineering, University of Science and Technology of China, Hefei 230026, China*

Ning Zhang − *State Key Laboratory of Rare Earth Resource Utilization, Changchun Institute of Applied Chemistry, Chinese Academy of Sciences, Changchun 130022, China; School of Applied Chemistry and Engineering, University of Science and Technology of China, Hefei 230026, China*

Jianrong Zeng − *Shanghai Synchrotron Radiation Facility, Shanghai Advanced Research Institute, Chinese Academy of Sciences, Shanghai 201204, China; Shanghai Institute of Applied Physics, Chinese Academy of Sciences, Shanghai 201800, China*

Complete contact information is available at: https://pubs.acs.org/10.1021/prechem.3c00101

Author Contributions

The manuscript was written through contributions of all authors.

Notes

The authors declare no competing financial interest.

■ ACKNOWLEDGMENTS

This work was supported by National Key R&D Program of China (2020YFE0204500). the National Natural Science Foundation of China (52273277, 52072362, 52071311), Jilin Province Science and Technology Development Plan Funding Project (20220201112GX), and Youth Innovation Promotion Association CAS (2020230 and 2021223). H.X.Z. thanks funding from National Natural Science Foundation of China Outstanding Youth Science Foundation of China (Overseas). These authors thank the staff of beamline BL13SSW at Shanghai Synchrotron Radiation Facility for experiments supports. The authors also gratefully appreciate the support of the morphology characterization and analysis from Prof. Jiuhui Han (Tianjin University of Technology).

■ REFERENCES

(1) De Luna, P.; Hahn, C.; Higgins, D.; Jaffer, S. A.; Jaramillo, T. F.; Sargent, E. H. What would it take for renewably powered electrosynthesis to displace petrochemical processes? *Science.* **2019**, *364* (6438), No. eaav3506.

(2) Wang, Y.; Liu, J.; Wang, Y.; Wang, Y.; Zheng, G. Efficient solar-driven electrocatalytic CO_2 reduction in a redox-medium-assisted system. *Nat. Commun.* **2018**, *9* (1), 5003−5010.

(3) Chen, C.; Khosrowabadi Kotyk, J. F.; Sheehan, S. W. Progress toward commercial application of electrochemical carbon dioxide reduction. *Chem.* **2018**, *4* (11), 2571−2586.

(4) Liu, S.-Q.; Wu, S.-W.; Gao, M.-R.; Li, M.-S.; Fu, X.-Z.; Luo, J.-L. Hollow porous Ag spherical catalysts for highly efficient and selective electrocatalytic reduction of CO_2 to CO. *ACS Sustain. Chem. Eng.* **2019**, *7* (17), 14443−14450.

(5) Zhu, W.; Michalsky, R.; Metin, Ö.; Lv, H.; Guo, S.; Wright, C. J.; Sun, X.; Peterson, A. A.; Sun, S. Monodisperse Au nanoparticles for selective electrocatalytic reduction of CO_2 to CO. *J. Am. Chem. Soc.* **2013**, *135* (45), 16833−16836.

(6) Gao, D.; Zhou, H.; Wang, J.; Miao, S.; Yang, F.; Wang, G.; Wang, J.; Bao, X. Size-Dependent electrocatalytic reduction of CO_2 over Pd nanoparticles. *J. Am. Chem. Soc.* **2015**, *137* (13), 4288−4291.

(7) Zhong, H.; Ghorbani-Asl, M.; Ly, K. H.; Zhang, J.; Ge, J.; Wang, M.; Liao, Z.; Makarov, D.; Zschech, E.; Brunner, E.; Weidinger, I. M.; Zhang, J.; Krasheninnikov, A. V.; Kaskel, S.; Dong, R.; Feng, X. Synergistic electroreduction of carbon dioxide to carbon monoxide on bimetallic layered conjugated metal-organic frameworks. *Nat. Commun.* **2020**, *11* (1), 1409−1418.

(8) Zhang, W.; Liu, S.; Yang, Y.; Qi, H.; Xi, S.; Wei, Y.; Ding, J.; Wang, Z. J.; Li, Q.; Liu, B.; Chen, Z. Exclusive Co-N_4 sites confined in two-dimensional metal-organic layers enabling highly selective CO_2 electroreduction at industrial-level current. *Angew. Chem., Int. Ed.* **2023**, *62* (23), No. e202219241.

(9) Wang, S.; Qian, Z.; Huang, Q.; Tan, Y.; Lv, F.; Zeng, L.; Shang, C.; Wang, K.; Wang, G.; Mao, Y.; Wang, Y.; Zhang, Q.; Gu, L.; Guo, S. Industrial-level CO_2 electroreduction using solid-electrolyte devices enabled by high-loading nickel atomic site catalysts. *Adv. Energy Mater.* **2022**, *12* (31), 2201278.

(10) Zhang, C.; Yang, S.; Wu, J.; Liu, M.; Yazdi, S.; Ren, M.; Sha, J.; Zhong, J.; Nie, K.; Jalilov, A. S.; Li, Z.; Li, H.; Yakobson, B. I.; Wu, Q.; Ringe, E.; Xu, H.; Ajayan, P. M.; Tour, J. M. Electrochemical CO_2 reduction with atomic iron-dispersed on nitrogen-doped graphene. *Adv. Energy Mater.* **2018**, *8* (19), 1703487.

(11) Zhang, Z.; Zhu, J.; Chen, S.; Sun, W.; Wang, D. Liquid fluxional Ga single atom catalysts for efficient electrochemical CO_2 reduction. *Angew. Chem., Int. Ed.* **2023**, *62* (3), No. e202215136.

(12) Li, M.; Wang, H.; Luo, W.; Sherrell, P. C.; Chen, J.; Yang, J. Heterogeneous single-atom catalysts for electrochemical CO_2 reduction reaction. *Adv. Mater.* **2020**, *32* (34), 2001848.

(13) Huang, J. R.; Qiu, X. F.; Zhao, Z. H.; Zhu, H. L.; Liu, Y. C.; Shi, W.; Liao, P. Q.; Chen, X. M. Single-product Faradaic efficiency for electrocatalytic of CO_2 to CO at current density larger than 1.2 A cm^{-2} in neutral aqueous solution by a single-atom nanozyme. *Angew. Chem., Int. Ed.* **2022**, *61* (44), No. e202210985.

(14) Chen, S.; Li, X.; Kao, C. W.; Luo, T.; Chen, K.; Fu, J.; Ma, C.; Li, H.; Li, M.; Chan, T. S.; Liu, M. Unveiling the proton-feeding effect in sulfur-doped Fe-N-C single-atom catalyst for enhanced CO_2 electroreduction. *Angew. Chem., Int. Ed.* **2022**, *61* (32), No. e202206233.

(15) Hossain, M. D.; Huang, Y.; Yu, T. H.; Goddard, W. A., Iii; Luo, Z. Reaction mechanism and kinetics for CO_2 reduction on nickel single atom catalysts from quantum mechanics. *Nat. Commun.* **2020**, *11* (1), 2256−2269.

(16) Ouyang, Y.; Shi, L.; Bai, X.; Li, Q.; Wang, J. Breaking scaling relations for efficient CO_2 electrochemical reduction through dual-atom catalysts. *Chem. Sci.* **2020**, *11* (7), 1807−1813.

(17) Zhu, J.; Xiao, M.; Ren, D.; Gao, R.; Liu, X.; Zhang, Z.; Luo, D.; Xing, W.; Su, D.; Yu, A.; Chen, Z. Quasi-covalently coupled Ni-Cu atomic pair for synergistic electroreduction of CO_2. *J. Am. Chem. Soc.* **2022**, *144* (22), 9661−9671.

(18) Li, Y.; Shan, W.; Zachman, M. J.; Wang, M.; Hwang, S.; Tabassum, H.; Yang, J.; Yang, X.; Karakalos, S.; Feng, Z.; Wang, G.; Wu, G. Atomically dispersed dual-metal site catalysts for enhanced CO_2 reduction: mechanistic insight into active site structures. *Angew. Chem., Int. Ed.* **2022**, *61* (28), No. e202205632.

(19) Zhao, R.; Wang, Y.; Ji, G.; Zhong, J.; Zhang, F.; Chen, M.; Tong, S.; Wang, P.; Wu, Z.; Han, B.; Liu, Z. Partially nitrided Ni nanoclusters achieve energy-efficient electrocatalytic CO_2 reduction to CO at ultralow overpotential. *Adv. Mater.* **2023**, *35* (5), 2205262.

(20) Yi, J. d.; Gao, X.; Zhou, H.; Chen, W.; Wu, Y. Design of Co-Cu diatomic site catalysts for high-efficiency synergistic CO_2 electroreduction at industrial-level current density. *Angew. Chem., Int. Ed.* **2022**, *61* (47), No. e202212329.

(21) Zeng, Z.; Gan, L. Y.; Bin Yang, H.; Su, X.; Gao, J.; Liu, W.; Matsumoto, H.; Gong, J.; Zhang, J.; Cai, W.; Zhang, Z.; Yan, Y.; Liu, B.; Chen, P. Orbital coupling of hetero-diatomic nickel-iron site for bifunctional electrocatalysis of CO_2 reduction and oxygen evolution. *Nat. Commun.* **2021**, *12* (1), 4088−4098.

(22) Hao, Q.; Zhong, H.-X.; Wang, J.-Z.; Liu, K.-h.; Yan, J.-m.; Ren, Z.-h.; Zhou, N.; Zhao, X.; Zhang, H.; Liu, D.-X.; Liu, X.; Chen, L.-W.; Luo, J.; Zhang, X.-B. Nickel dual-atom sites for electrochemical carbon dioxide reduction. *Nat. Synth.* **2022**, *1* (9), 719−728.

(23) Zhang, L.; Feng, J.; Liu, S.; Tan, X.; Wu, L.; Jia, S.; Xu, L.; Ma, X.; Song, X.; Ma, J.; Sun, X.; Han, B. Atomically dispersed Ni-Cu catalysts for pH-universal CO_2 electroreduction. *Adv. Mater.* **2023**, *35* (13), 2209590.

(24) Hao, Q.; Tang, Q.; Zhong, H.-X.; Wang, J.-Z.; Liu, D.-X.; Zhang, X.-B. Fully exposed nickel clusters with electron-rich centers for high-performance electrocatalytic CO_2 reduction to CO. *Sci. Bull.* **2022**, *67* (14), 1477−1485.

(25) Liu, C.; Wu, Y.; Sun, K.; Fang, J.; Huang, A.; Pan, Y.; Cheong, W.-C.; Zhuang, Z.; Zhuang, Z.; Yuan, Q.; Xin, H. L.; Zhang, C.; Zhang, J.; Xiao, H.; Chen, C.; Li, Y. Constructing FeN_4/graphitic nitrogen atomic interface for high-efficiency electrochemical CO_2 reduction over a broad potential window. *Chem.* **2021**, *7* (5), 1297−1307.

(26) Chen, J.; Wang, D.; Yang, X.; Cui, W.; Sang, X.; Zhao, Z.; Wang, L.; Li, Z.; Yang, B.; Lei, L.; Zheng, J.; Dai, L.; Hou, Y. Accelerated transfer and spillover of carbon monoxide through tandem catalysis for kinetics-boosted ethylene electrosynthesis. *Angew. Chem., Int. Ed.* **2023**, *62* (10), 2209590.